J Solid State Electrochem (2012) 16:1683–1692
DOI 10.1007/s10008-011-1577-3

ORIGINAL PAPER

Construction of hyaluronan-silver nanoparticle–hemoglobin multilayer composite film and investigations on its electrocatalytic properties

Fei Zhang · Juan Wu · Hongbin Zhang

Received: 8 July 2011 / Revised: 15 September 2011 / Accepted: 16 October 2011 / Published online: 12 November 2011

Abstract In this work, hyaluronan-silver nanoparticles (HSNPs) were prepared by UV-initiated photoreduction, and protein hemoglobin (Hb) was then alternately assembled with the prepared negatively charged HSNPs into layer-by-layer (LBL) films on solid surface. The electrochemical behavior and electrocatalytic activities toward oxygen and hydrogen peroxide of the resulting films were studied. It was found that the HSNPs greatly enhanced the electron transfer reactivity of Hb as a bridge. The assembly films showed a pair of nearly reversible redox peaks with a formal potential of −0.32 V (vs. Ag/AgCl) for the heme Fe(III)/Fe(II) redox couple. The immobilized Hb in the films maintained its biological activity, showing a surface-controlled process with a heterogeneous electron transfer rate constant (k_s) of 1.0 s^{-1} and displaying the same features of a peroxidase in the electrocatalytic reduction of oxygen and hydrogen peroxide. This work provides a novel model to fabricate LBL films with protein, polysaccharide and nanoparticles, which may establish a foundation for fabricating new type of biosensors based on the direct electron transfer of redox proteins immobilized in nanocomposite multilayer films with underlying electrodes.

Keywords Hemoglobin · Hyaluronan · Silver nanoparticle · Layer-by-layer assembly · Enzymatic catalysis

F. Zhang · J. Wu · H. Zhang (✉)
Department of Polymer Science and Engineering,
School of Chemistry and Chemical Engineering,
Shanghai Jiao Tong University,
Shanghai 200240, China
e-mail: hbzhang@sjtu.edu.cn

Introduction

Much attention has been paid to the research on direct electron transfer of redox proteins or enzymes with electrodes recently because it can provide a model system for understanding the complicated electron transfer mechanism in real biological systems and establish a foundation for constructing the third-generation biosensor and bioelectronics [1–3]. However, it is difficult for some redox proteins to exchange electrons directly with bare solid electrodes. In recent decades, the immobilization of proteins into ultrathin films modified on electrode surface has attracted more attentions because of its realization of the direct electrochemistry of proteins [4–6]. Among the methods of fabrication of these ultrathin films, layer-by-layer (LBL) technique has been the most commonly used because of its remarkable nano-scale control, simplicity, and versatility in the assembly [7].

Hemoglobin (Hb), a typical multi-cofactor protein [8], is considered to be an ideal model protein for the study of the electron transfer of heme molecules because of its commercial availability, moderate cost, well-known, and documented structure as well as enzyme-like oxidative and reductive catalytic activity [9]. However, it has been found that on conventional solid electrodes, the fast electron transfer between Hb and the electrode is not possible because the redox center of proteins is embedded in polypeptide chain structures and the proteins are easily absorbed on the electrode surface [10]. Varied support materials such as clay [11], ion liquid films [12], and nanomaterial [13] are used to promote the electron transfer and maintain the enzymatic activity. Among these materials, silver nanoparticles have gained considerable attentions due to their easy syntheses, large specific area, conductivity, antibacterial properties, and high catalytic activity [14–

16]. They can provide a microenvironment similar to that of the redox proteins in native systems and therefore are widely used in constructing electrochemical biosensors. For example, Gu et al. [17] fabricated Hb-colloidal silver nanoparticles (CSNs)-chitosan film on the glassy carbon electrode (GCE) and explored its potential application on electrochemical biosensing. Sun and co-workers [18] constructed a biosensor by entrapping Hb/CSNs in titania sol–gel matrix on GCE by a vapor deposition method.

Hyaluronan (HA) is a natural linear, unbranched polyanion which is composed of a repeating disaccharide consisting of *N*-acetyl-D-glucosamine and D-glucuronic acid alternately linked by β 1–4 and β 1–3 glycosidic bond. HA is the important component of the extracellular matrix and pericellular matrix and has the multiple physiological function and excellent physicochemical properties [19–21]. Due to these properties, HA has been extensively used in LBL assemblies, mostly together with poly(allylamine) [22], polylysine [23] forming self-assembled films mainly used in drug delivery. Liu and Hu [24] reported the formation of $[HA/Mb]_n$ film on pyrolytic graphite and explored the electrochemistry of the protein in the assembly films. Brett et al. [25] systemically studied the electrochemical properties of the HA/Mb assembly films on the gold electrode.

For the biosensors used in detection in vivo, properties such as biocompatibility, antibacterial properties, and stability are essential [26–28]. Therefore, the assembly multilayer films combining the biocompatibility of HA, antibacterial property of silver nanoparticle alone with enzyme-like catalytic activity of Hb may be of potential applications in biosensing in vitro and in vivo. To our knowledge there are few work done for the construction and investigation on the electrocatalytic activities of HA-silver nanoparticle–Hb assembly multilayer films on the glass carbon electrode. In the present work, the HA-silver nanoparticles (HSNPs) were prepared by UV-initiated photoreduction and alternately assembled with Hb into LBL films on the glass carbon electrode. The electrocatalytic properties of the ultrathin films were investigated and discussed.

Experimental

Reagents and materials

Bovine Hb (M_w, 68 kDa) was obtained from Boao Biotechnology Co., Ltd (Shanghai, China). HA (M_w, 1,500 kDa) was supplied from Shandong Freda Biopharm Co., Ltd (China). Polyethyleneimine (PEI, 50%; M_w, 70 000) was obtained from Aladdin Reagent Co., Ltd (China). Buffer used in this work was 0.05 M acetate (pH=5), and 0.1 M sodium dihydrogen phosphate (pH 5–11), whose pH values were adjusted with HNO_3 or NaOH solutions. Silver nitrate ($AgNO_3$) was supplied by Sinopharm Chemical Reagent Co., Ltd (China). Water was purified by successive ion exchange and distillation. All the other chemicals are of reagent grade.

HA-silver nanoparticles preparation

Silver nanoparticles were prepared according to the method described by Li et al. [29] with minor modification. Briefly, $AgNO_3$ (0.6 mL and 100 mM), HA (2 mL and 10 mg/mL), and ultrapure water (7.4 mL) were mixed in a bottle for a final concentration of 6 mM $AgNO_3$+2 mg/mL HA. The solution was then irradiated with UV light (wavelength at 365 nm) by ultraviolet lamp (12 W, ZF7, Shanghai Yuying Industrial Co., China), for 10 h. After that, the solution was centrifuged at 12,000 rpm for 30 min and then the sediment obtained from removal of the supernatant was repeatedly purified three times by resuspending the sediment in water and recentrifuging it. The nanoparticles were finally collected by lyophilization.

Film assembly

The assembly process of the multilayer composite films on solid substrates was schematically shown in Scheme 1. For electrochemical study, GCE (3 mm in diameter) was used as the working electrode. Prior to use, GCE was polished carefully with 1.0, 0.3, and 0.05 μm alumina slurry, respectively. After rinsing thoroughly with twice-distilled water, it was sonicated in absolute ethanol and twice-distilled

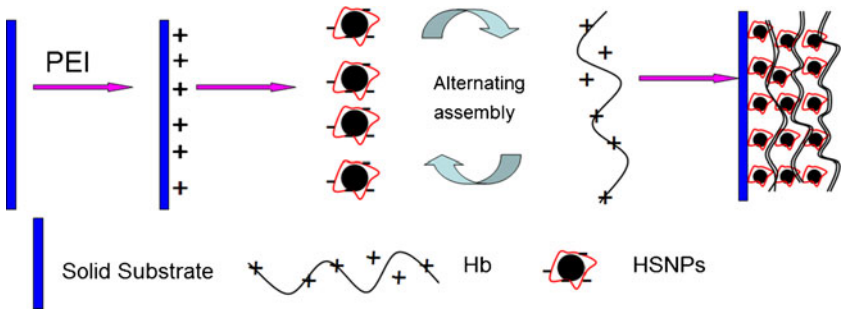

Scheme 1 Schematic of the HA-silver nanoparticles (*HSNPs*) and hemoglobin (*Hb*) multilayer film build up on solid substrate

water for about 1 min, respectively. A precursor monolayer of positively charged PEI was adsorbed by immersing the GCE into 3 mg/mL PEI in 0.05 M acetate solutions+0.2 M $NaNO_3$ at pH 5.0 solution for 20 min. After that, the electrode was carefully washed and dried in a N_2 stream. The GCE/PEI electrode was then alternately immersed into the HA-silver nanoparticle (1 mg/ml HA, 3 mM silver nanoparticles) in 0.05 M acetate solutions+0.2 M $NaNO_3$ at pH 5.0 solution and Hb in 0.05 M acetate solutions (1 mg/mL, containing 0.2 M $NaNO_3$ at pH 5.0) for 20 min with intermediate water washing and N_2 drying. The build-up process was carried out until a desired number (n) of bilayers denoted as $[HAS/Hb]_n$ was deposited on the electrode substrates. The assembly films of HA and Hb, denoted as $[HA/Hb]_n$, were also constructed on the GCE by the same method.

For ultraviolet–visible (UV–vis) spectroscopic study, a quartz slide (1×4 cm and 1 mm thick) was firstly immersed into a freshly prepared "piranha solution" (3:7 volume ratio of 30% H_2O_2 and 98% H_2SO_4) for 20 min, rinsed carefully with water, and then dried with a nitrogen stream. This made the slide surface become positive. The $[HAS/Hb]_n$ films were assembled on the quartz slides with the same procedure as that of the CGE. For comparison, the assembly films of $[HA/Hb]_n$, were also constructed by the same method.

Measurements and apparatus

Electrochemical measurements were performed with a CHI 604B electrochemical workstation (CH Instruments Co., USA) using the modified GCE as the working electrode, a platinum wire as the counter and a Ag/AgCl electrode as reference electrode. Before electrochemical measurements, 0.1 M, pH= 7 PBS solutions were purged with purified nitrogen for at least 15 min. A nitrogen atmosphere was then kept in the cell by continuously bubbling N_2 during the whole experiment. The UV–vis spectra were recorded on an UV-2450 spectrophotometer (Shimadzu, Japan). The average size and morphology of HSNPs were observed by a JEM-2010HR transmission electronmicroscope (TEM). Scanning electron microscopy (SEM) photographs of various assembly ultrathin films were recorded with a Hitachi 8100 instrument at 200 kV. Prior to SEM analysis, the films on quartz slide were coated by thin gold films with an E-1045 ion sputter (Hitachi, Japan). All experiments were performed at ambient temperature (20±2 °C). Zeta potential of the HSNPs was measured by a Malvern Nano ZS90 (Malvern Instruments, UK).

Results and discussion

Characterization of HSNPs and morphology of HSNPs–Hb multilayer films

HSNPs were successfully prepared in situ through UV-initiated photoreduction verified by UV–vis adsorption spectrum and TEM images as shown in Fig. 1a, b. Figure 1a shows the UV–vis absorption of the silver particles, which was characterized by the absorption at 447 nm in the visible region. Both the particle size and shape have been further observed by TEM shown in Fig. 1b. It could be observed that the particles were well dispersed with spherical shapes of 30–60 nm. The zeta

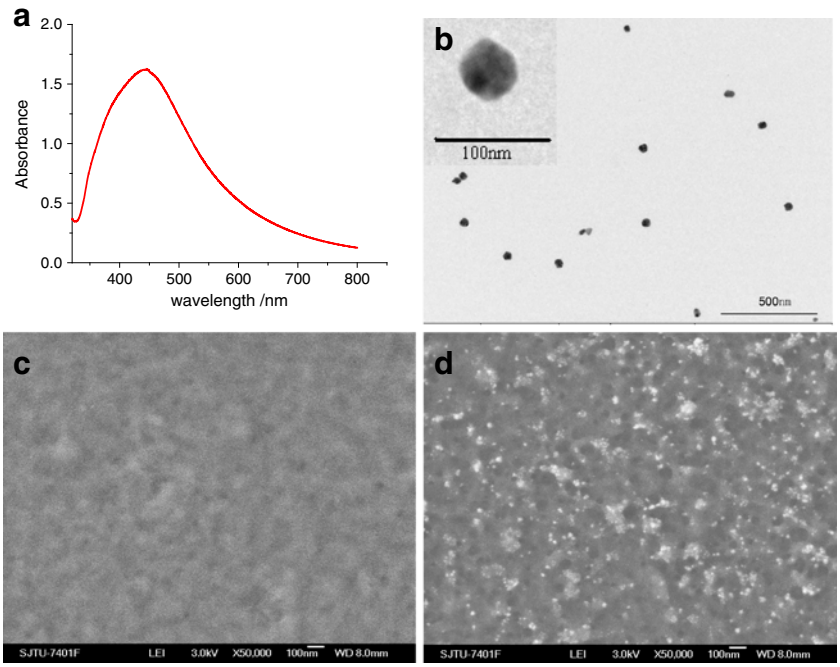

Fig. 1 **a** UV–vis absorption spectrum, **b** TEM image of HSNPs, **c** SEM image of $[HA/Hb]_6$ film, and **d** SEM image of $[HAS/Hb]_6$ film

potential of the resulting silver nanoparticles was found to be −40.47 mV that indicated the HSNPs carried negative surface charges. While HSNPs stabilized by HA carried negative surface charges, Hb, with an isoelectric point at pH 7.0–7.4 [30, 31], had considerable positive surface charges at pH 5.0. Thus, LBL films of HA/Hb and HSPNs/Hb at pH 5.0 can be assembled on different substrates through electrostatic interaction between them. The surface morphologies of $[HA/Hb]_6$ and $[HAS/Hb]_6$ with Hb as the outermost layer were shown in Fig. 1c, d, respectively. In comparison with Fig. 1c, a large number of silver nanoparticles were observed distributing uniformly on the surface of $[HAS/Hb]_6$ (Fig. 1d). The sizes of the nanoparticles were ca. tens of nanometers, which were in the same order as observed in TEM (Fig. 1b). The HSNPs around the Hb or connected with Hb should provide a microenvironment similar to that of the redox proteins in native systems, and were beneficial to the direct electron transfer of Hb [18]. In addition, the surface morphology of the $[HAS/Hb]_6$ film (Fig. 1d), presented porous structures, similar to that of CSNs-chitosan film [17]. These unique porous structures might facilitate access of substrates to the bound proteins [17].

Characterization of the LBL assembly HSNPs–Hb multilayer

Hb has a strong Soret absorption band for its heme groups at about 410 nm [32], and HSNPs have a comparative strong absorption at about 447 nm (Fig. 1a). Therefore UV–vis spectroscopy could be used to monitor the growth of LBL films on quartz slides with a precursor of PEI on the surface. Figure 2a and b present the UV–vis spectroscopy of different bilayers of $[HA/Hb]_n$ and $[HAS/Hb]_n$, respectively. The UV–vis spectra at consecutive cycles of the adsorption of HA/Hb and HAS/Hb bilayer on quartz slides showed that the Soret absorption band at 411 nm increased with the number of bilayers. The difference of the two films was that in the UV–vis spectroscopy of the $[HAS/Hb]_n$ (Fig. 2b), there was apparent absorption at 447 nm corresponding to the absorption of HSNPs which has been shown in Fig. 1a. This confirmed the successful assembly of $[HAS/Hb]_n$ films on quartz slides. The similar positions of Soret band of Hb in $[HAS/Hb]_n$ films and in the Hb solution also indicated that the Hb in the LBL films essentially retained its native structure.

Cyclic voltammetry (CV) was also used to monitor the fabrication of $[HAS/Hb]_n$ films on GCE (Fig. 3). After alternate absorption of HSNPs and Hb and the formation of the first bilayer, a pair of nearly reversible reduction–oxidation peaks was observed at about −0.32 V vs. Ag/AgCl, characteristic of the Hb heme Fe (III)/Fe(II) redox couple [33]. With the increase of the number of bilayers, both reduction and oxidation peaks increased. For n close to 6, the peak currents kept nearly constant and did not increase further, indicating that Hb molecules assembled in the bilayers with n larger than 6 were no longer electrochemically accessible which has also been found by He and Hu [32].

Direct electrochemical behavior of Hb on $[HAS/Hb]_6$ films/GCE

Cyclic voltammograms of differnt films-modified GCE were recorded in 0.1 M PBS at pH 7.0. As shown in Fig. 4, while no CV peaks were observed on a bare GC electrode (curve a), for $[HAS/Hb]_6$ films (curve c), a couple of stable and well-defined redox peaks at −0.28 and −0.35 V, respectively, was observed. The potential separation ΔE_p was about 70 mV, which is the characteristic of heme FeIII/FeII redox couple of the protein [17, 18, 34]. When Hb was immobilized in $[HA/Hb]_6$ film in the absence of silver nanoparticles, the CV showed a comparatively small response of Hb (curve b), indicating that $[HAS/Hb]_6$ film containing silver nanoparticles (curve c) was much more favorable to the direct electron transfer of Hb. In fact, HSNPs could reduce the insulating property of the protein shell for the direct electron transfer and play the role of an efficient electron-conducting tunnel [35]. Furthermore, the strong adsorption of silver nanoparticles to Hb might

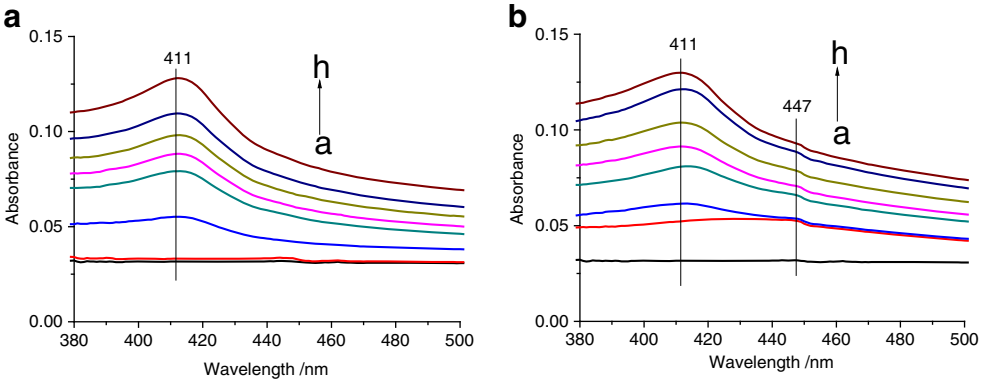

Fig. 2 UV–vis spectra of $[HA/Hb]_n$ (**a**) and $[HAS/Hb]_n$ (**b**) films grown on the quartz/PEI surface with different numbers of bilayers (n). **a** PEI layer (a); PEI/HA bilayer (b); $[HA/Hb]_n$ (n=1–6) (c–h); **b** PEI layer (a); PEI/HAS bilayer (b); $[HAS/Hb]_n$ (n=1–6) (c–h)

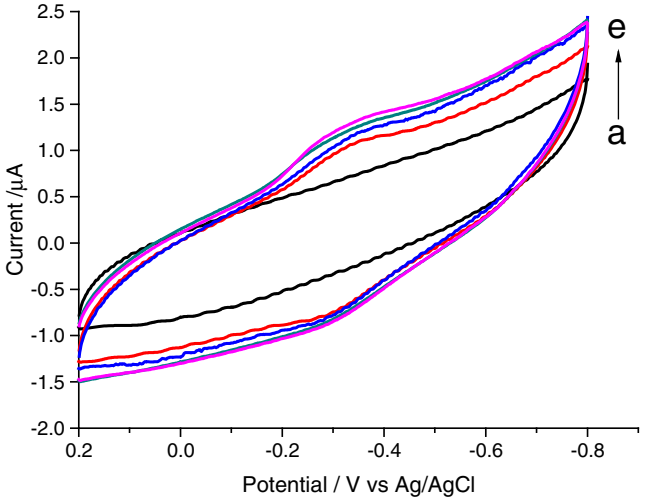

Fig. 3 Cyclic voltammograms of $[HAS/Hb]_n$ films assembled on GCE in 0.1 M at pH 7.0 PBS at 50 mV/s. (*a–e* bare GC, bilayer 1, bilayer 2, bilayer 4, and bilayer 6)

reduce the denaturation of Hb on GCE and caused adsorbed protein to possess a favorable orientation for the direct electron transfer between Hb and GCE [36].

Figure 5 presents the cyclic voltammograms of the $[HAS/Hb]_6$ films/GCE at different scan rates. The redox peak currents increased linearly with the scan rate between 50 and 300 mV/s (Fig. 5 inset), as expected for a thin-layer electrochemical behavior. In addition, the cathodic peak currents were almost the same as the corresponding anodic peak currents accompanied slightly enlarged peak-to-peak separation (ΔE_p). These results are characteristic of quasi-reversible, surface-confined electrochemical behavior in which all electroactive proteins in the films reduce to ferrous hemoglobin Hb–Fe(II) on the forward cathodic scan, and the Hb–Fe(II) produced is reoxidized to Hb–Fe (III) on the reverse scan [18].

Based on the Faraday's law [37], the electroactive Hb amount (mol/cm^2) on the electrode surface, Γ^*, could be expressed as

$$\Gamma^* = Q/(nFA) \tag{1}$$

where Q is the quantity of charge (C) that can be obtained through the integration of the CV reduction peak, n is the charge transfer number, F is Faraday's constant, and A the geometrical surface area of electrode. The value of Γ^* in our work was calculated to be 5.23×10^{-11} mol/cm^2. This value is larger than that of the Hb in the agarose hydrogel and room temperature ionic liquid composite films (2.30×10^{-11} mol/cm^2) [38], in the (Fe_3O_4/chitosan–phytic acid)$_4$ film (4.24×10^{-11} mol/cm^2) [39], and much larger than that of theoretical monolayer coverage of the Hb (1.89×10^{-11} mol/cm^2) [40], indicating that Hb saturated adsorbed onto the assembly films with multilayer coverage [41].

According to Laviron equation [42], the peak current (in μA), I_p, could be expressed as follows:

$$I_P = \frac{n^2F^2A\Gamma^*v}{4RT} = \frac{nFQv}{4RT} \tag{2}$$

where v is the scan rate, R gas constant, and T the temperature. From the slope of the I_p vs. v, n was calculated to be 1.06. Therefore, the redox of Hb in the assembly films is a single electron transfer reaction.

When $n\Delta E_p \leq 0.2$ V, the electron transfer rate constant (k_s) of the Hb in $[HAS/Hb]_6$ film could be estimated by the following equation [43]:

$$\log k_s = \alpha\log(1-\alpha) + (1-\alpha)\log\alpha - \log\frac{RT}{nFv} - \frac{\alpha(1-\alpha)nF\Delta E_p}{2.3RT} \tag{3}$$

Taking the electron transfer coefficient α of 0.5, a scan rate of 100 mV/s, and the ΔE_p of 70 mV, the rate constant could be estimated to be 1.0 s^{-1}. This value is in the controlled range of surface-controlled quasi-reversible process, and it is larger than those reported for Hb immobilized on polymer-MWNT-modified GCE (0.4 s^{-1}) [44], indicating a fairly fast electron transfer between the immobilized Hb and GCE.

Figure 6 shows cyclic voltammograms of $[HAS/Hb]_6$/GCE at different pH values. An increase in solution pH value caused a negative shift in potentials for both reduction and oxidation peaks for the modified electrode (Fig. 6a). In addition, as shown in Fig. 6b, the formal potential shifted negative linearly with the increase of pH from 5.0 to 10.8. The reason might be the change in the protonation of a water molecule at the sixth coordination position in

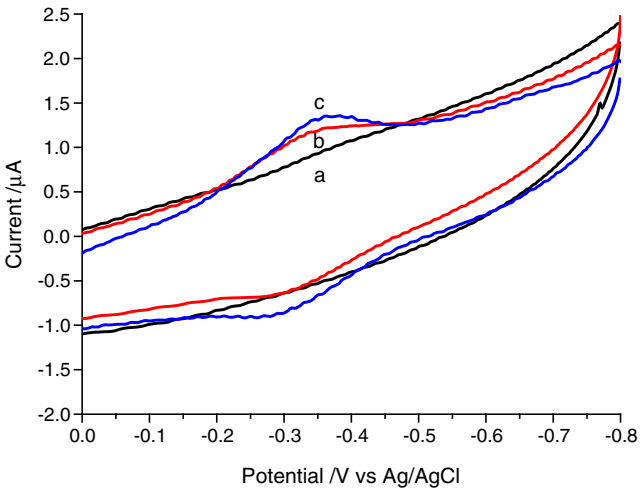

Fig. 4 Cyclic voltammograms of *a* bare GCE, *b* $[HA/Hb]_6$-modified GCE, *c* $[HAS/Hb]_6$-modified GCE in 0.1 M at pH 7.0 PBS. Scan rate, 50 mV/s

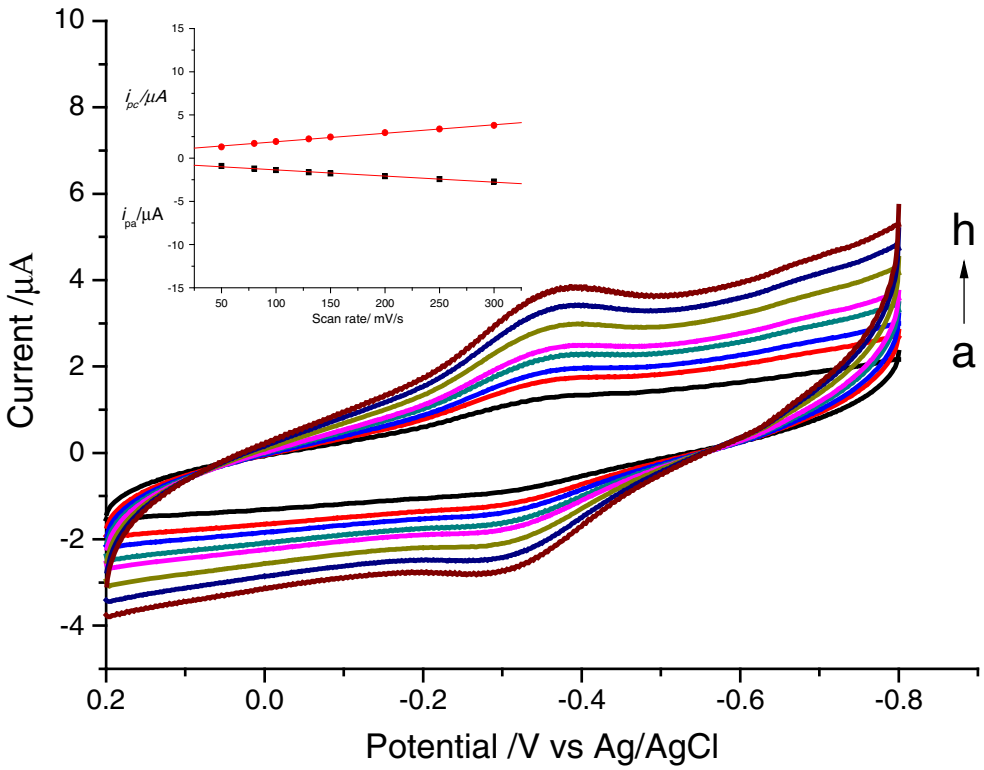

Fig. 5 Cyclic voltammograms of $[HAS/Hb]_6$/GCE in pH 7.0 PBS with the scan rates from inner to outer as 50, 80, 100, 130, 150, 200, 250, and 300 mV/s, respectively. *Inset*, linear relationship of the peak current vs. the scan rate

the heme iron and also protonation of the protolytic groups around the heme with changing pH [45]. The slop of the plot was −41.56 mV/pH, smaller than the expected theoretical value of 57.6 mV/pH for a single-proton coupled to one-electron transfer for each heme group of Hb during the reversible electrode reaction [46]. The fact may be due to the effect of the protonization of ligands to the heme iron and amino acids around the heme [47]. In addition, the negative shift in formal potential may also reflect the change in the hydrophobic-hydrophilic nature of the microenvironment in films [48].

Electrocatalysis of HA-silver nanoparticle–Hb films-modified GC electrode

As reported, heme proteins are able to catalyze the reduction of various substances including O_2, H_2O_2, NO, and so on [49, 50]. Here, we choose O_2 and H_2O_2 as substrates to study the electrochemical catalytic activity of Hb in $[HAS/Hb]_6$ films.

The electrocatalytic property of the $[HAS/Hb]_6$ film toward oxygen was investigated by CV shown in Fig. 7. When a certain amount of air was injected into oxygen-free at pH 7.0 PBS solution using a syringe, a significant increase in reduction peak was observed at about −0.4 V. On the other hand, the oxidation peak of Hb FeIII/FeII redox couple nearly disappeared. An increase in the amount of air in solution resulted in the increase of the reduction peak current. These behaviors implied that Hb immobilized on the assembly ultrathin film had a satisfactorily catalytic activity toward O_2.

Electrochemical catalytic reductions of hydrogen peroxide using $[HAS/Hb]_6$ films/GCE are shown in Fig. 8a. When H_2O_2 was added into pH 7.0 buffers, an increase in

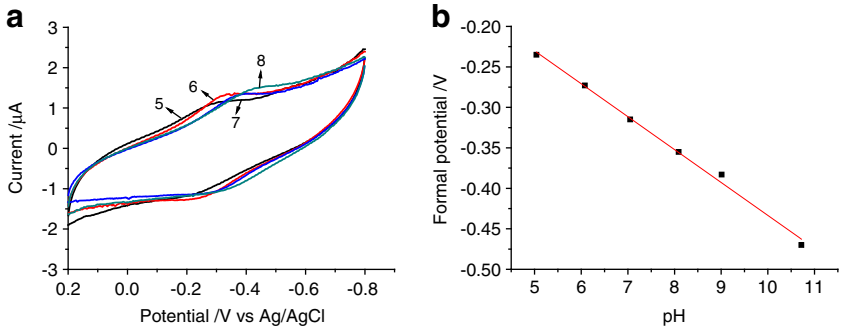

Fig. 6 **a** Cyclic voltammograms of $[HAS/Hb]_6$/GCE at a scan rate of 50 mV/s in PBS with different pH values of 5.0, 6.0, 7.0, and 8.0. **b** The linear plot of the formal potentials vs. pH

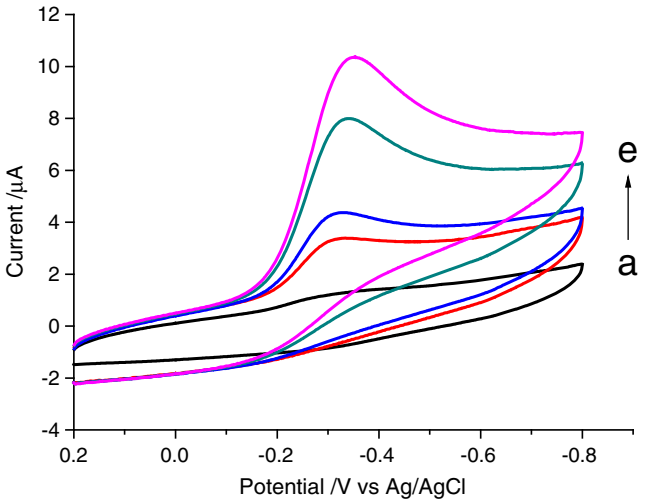

Fig. 7 Cyclic voltammograms of $[HAS/Hb]_6$/GCE in 0.1 M at pH 7.0 PBS containing *a* 0-, *b* 5-, *c* 10-, *d* 30-, and *e* 50-ml air. Scan rate, 50 mV/s

the reduction peak at about −0.4 V for $[HAS/Hb]_6$ films was observed with the decrease of the oxidation peak. These results further confirmed that our $[HAS/Hb]_6$ film was a friendly platform for the immobilization of Hb and had a good electrocatalysis to H_2O_2. Figure 8b shows the relationship between the electrocatalytic current and the concentration of H_2O_2. The electrocatalytic current was obtained by deducting anionic peak current of the PBS without hydrogen peroxide from the anionic peak current of the PBS containing the certain concentration of hydrogen peroxide [51]. A linear dependence of the electrocatalytic current on the concentration of H_2O_2 was observed in the range of 0.7 to 75 μM with a correlation coefficient of 0.9985 (Fig. 8b). At higher H_2O_2 concentrations, the CV responses showed a level-off tendency and then fell down. This is characteristic of the enzyme catalyzed reaction [51]. A linear regression equation was obtained as $I_{cat}(\mu A) = 0.031\, C_{H_2O_2}(\mu M) + 0.02$, with a correlation coefficient of 0.991.

The characteristics of sensitivity and response time of biosensor are important for its applications [52, 53]. Here these properties were investigated through the amperometric response of the $[HAS/Hb]_6$ films/GCE to H_2O_2 at applied potential −0.4 V as shown in Fig. 9. The stepped increase of H_2O_2 concentration in buffers caused the corresponding growth of reduction currents for $[HAS/Hb]_6$ films, and the 95% of the steady-state current was achieved in less than 4 s. The obtained calibration curve demonstrated a linear range of 6–90 μM with LOD (Limit of Detection) of 0.6 μM (*S/N*=3) and correlation coefficient of 0.995. The response slop is 7.9 μA mM^{-1}, which is larger than those obtained for Hb incorporated in polytetrafluoroethylene film cast on GCE (6.6 μA mM^{-1}) [54] and for Hb immobilized on CSNs-chitosan film-modified GCE (1.85 μA mM^{-1}) [17], indicating a reasonably high sensitivity of the constructed biosensor.

The selectivity of this biosensor was evaluated by H_2O_2 determinations in the presence of some potentially coexisting compounds of H_2O_2 in biological systems. In our experiment, some interfering substances including glucose, uric acid, dopamine, and several cations such as Cu^{2+}, Mg^{2+}, and Zn^{2+} were tested. When the tolerance limit was defined as the concentration ratio of additive/H_2O_2 causing less than 5.0% relative error, it was found that for the determination of 50 μM H_2O_2, 20-fold of Cu^{2+}, Mg^{2+}, Zn^{2+}, glucose, uric acid, and dopamine, did not cause significant interferences. The Hb in the assembly films can exhibit selectivity to detect H_2O_2.

The reproducibility of the response of the enzyme electrode was investigated in 0.1 M at pH 7.0 PBS solution containing 50 μM H_2O_2. The relative standard deviation determined with the same enzyme electrode was found to be 1.17% (experimental number, 5). The stability of the biosensor under storage in PBS at 4 °C was also investigated by measuring the biosensor response to 50 μM of H_2O_2 in 0.1 M at pH 7.0 PBS solution. In comparison to the initial film-modified electrode, the electrode exhibited no changes in CV peak potential and

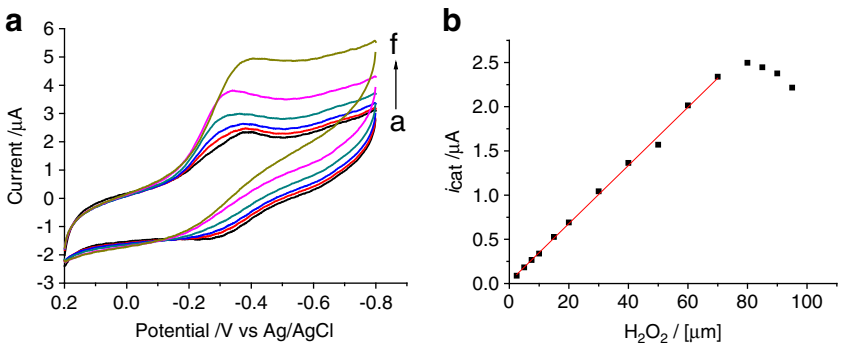

Fig. 8 **a** Cyclic voltammograms of $[HAS/Hb]_6$/GCE in 0.1 M at pH 7.0 PBS containing *a* 0, *b* 5, *c* 10, *d* 20, *e* 40, and f 80 μM H_2O_2. Scan rate, 100 mV/s. **b** Plot of catalytic peak current versus concentration of H_2O_2 in 0.1 M at pH 7.0 PBS. Scan rate, 100 mV/s

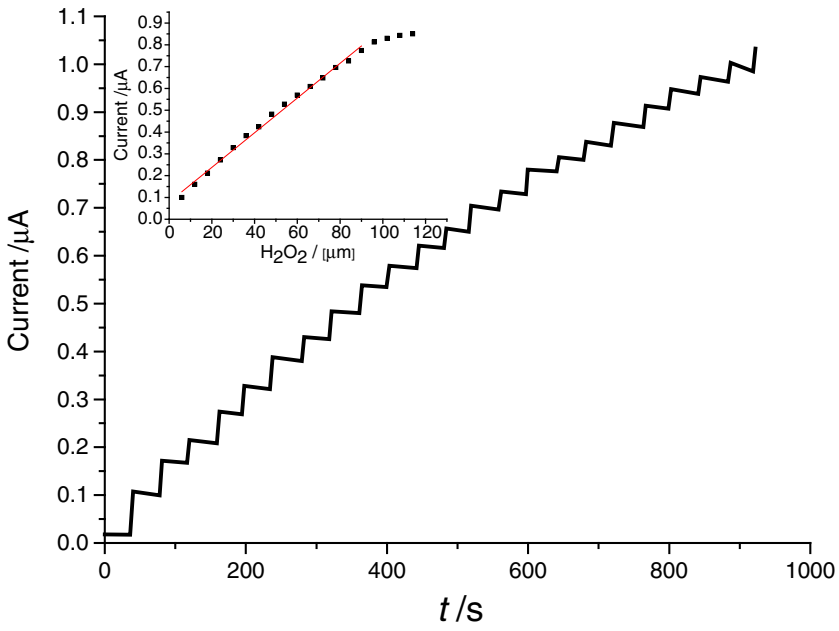

Fig. 9 Amperometric current–time curve at the constant potential of −0.4 V vs. Ag/AgCl in pH 7.0 PBS with successive additions of 6 μM H_2O_2 for $[HAS/Hb]_6$/GCE. *Inset*, amperometric response curve for H_2O_2

only a slight decrease in peak current (within 10%) in 30 days, showing a good stability.

The H_2O_2 detection performances of the proposed biosensor were compared with those of other enzymatic biosensors based on different matrices and the results were shown in Table 1. It can be seen that the $[HAS/Hb]_6$/GCE offered reasonable linear range for H_2O_2 detection, comparatively high sensitivity and good stability. These indicated that the proposed biosensor was a good platform for the detection of H_2O_2

Conclusions

In this work, Hb was successfully immobilized on GCE through layer-by-layer assembly of Hb and HSNPs. The presence of HSNPs provided the Hb molecules effective adsorption sites on which their active centers could be easily accessed so that the direct electron transfer of Hb was significantly promoted. Hb in the $[HAS/Hb]_6$ films fabricated on GCE retained its original structure and showed good direct electrochemistry and electrocatalytic reactivity toward oxygen and hydrogen peroxide. This work provides a novel model to fabricate LBL films with protein, polysaccharide and nanoparticles. The direct electron transfer and electrocatalytic activity of redox enzymes can be promoted in this kind of nanocomposite multilayer films. The unique properties, non-toxicity of the formed HSNPs combined with the biocompatibility and multiple physiological function of HA may make the constructed biosensor more suitable to be applied in vivo detection.

Table 1 Comparison of performances of proposal biosensor for H_2O_2 detection with those of other enzymatic biosensors

Electrode	Respond time (s)	Linear range (μM)	Stability[a]	Reference
Hb/graphene–chitosan film/GCE	Within 5	6.5–230	80.1% for 14 days	[55]
Hb/poly(ε-caprolactone) film/GCE	NA	2–30	90% for 14 days	[56]
Hb–CSNs–chitosan/GCE	Within 4	0.75–216	95% for 15 days	[17]
Mb–CGNs–Nafion/GCE	Within 5	1.5–90	93% for 50 days	[2]
Hb/titania sol–gel film/GCE	Within 5	0.5–54	89% for 80 days	[57]
HRP/polyion complex membrane GCE	Within 15	0.5–10	80% for 30 days	[58]
Hb/$[HAS/Hb]_6$/GCE	Within 4	6–90	90% for 30 days	This paper

CSNs colloid silver nanoparticle, *CGNs* colloid gold nanoparticles, *Mb* myoglobin, *HRP* horseradish peroxidase

[a] The stability was evaluated by the percent of retaining its initial current response of the biosensor stored in PBS at 4 °C for some days

Acknowledgments The authors are thankful for the financial support for this work from the National Natural Science Foundation of China (grant no. 21074071) and the Shanghai Leading Academic Discipline Project (no. B202).

References

1. Bullen RA, Arnot TC, Lakeman JB, Walsh FC (2006) Biofuel cells and their development. Biosens Bioelectron 21(11):2015–2045
2. Yang W, Li Y, Bai Y, Sun C (2006) Hydrogen peroxide biosensor based on myoglobin/colloidal gold nanoparticles immobilized on glassy carbon electrode by a Nafion film. Sens Actuators, B 115 (1):42–48
3. Gao R, Shangguan X, Qiao G, Zheng J (2008) Direct electrochemistry of hemoglobin and its electrocatalysis based on hyaluronic acid and room temperature ionic liquid. Electroanalysis 20(23):2537–2542
4. Rusling JF (1998) Enzyme bioelectrochemistry in cast biomembrane-like films. Acc Chem Res 31(6):363–369
5. Lvov Y, Möhwald H (2000) Protein architecture: interfacing molecular assemblies and immobilization biotechnology. Marcel Dekker, NewYork
6. He P, Hu N, Rusling JF (2003) Driving forces for layer-by-layer self-assembly of films of SiO2 nanoparticles and heme proteins. Langmuir 20(3):722–729
7. Pinto EM, Barsan MM, Brett CMA (2010) Mechanism of formation and construction of self-assembled myoglobin/hyaluronic acid multilayer films: an electrochemical QCM, impedance, and AFM study. J Phys Chem B 114(46):15354–15361
8. Mai Z, Zhao X, Dai Z, Zou X (2010) Direct electrochemistry of hemoglobin adsorbed on self-assembled monolayers with different head groups or chain length. Talanta 81(1–2):167–175
9. Yu J-J, Zhao F-Q, Zeng B-Z (2008) Characterization and electrochemical study of hemoglobin–carbon nanoparticles–polyvinyl alcohol nanoporous hybrid film. J Solid State Electrochem 12(9):1167–1172
10. Heller A (1990) Electrical wiring of redox enzymes. Acc Chem Res 23(5):128–134
11. Charradi K, Forano C, Prevot V, Ben Haj Amara A, Mousty C (2009) Direct electron transfer and enhanced electrocatalytic activity of hemoglobin at iron-rich clay modified electrodes. Langmuir 25(17):10376–10383
12. Lu X, Hu J, Yao X, Wang Z, Li J (2006) Composite system based on chitosan and room-temperature ionic liquid: direct electrochemistry and electrocatalysis of hemoglobin. Biomacromolecules 7(3):975–980
13. Wen Y, Wu H, Chen S, Lu Y, Shen H, Jia N (2009) Direct electrochemistry and electrocatalysis of hemoglobin immobilized in poly(ethylene glycol) grafted multi-walled carbon nanotubes. Electrochim Acta 54(27):7078–7084
14. Zheng J, Chumanov G, Cotton TM (2001) Photoinduced electron transfer at the surface of nanosized silver particles as monitored by EPR spectroscopy. Chem Phys Lett 349(5–6):367–370
15. Liu T, Zhong J, Gan X, Fan C, Li G, Matsuda N (2003) Wiring electrons of cytochrome c with silver nanoparticles in layered films. ChemPhysChem 4(12):1364–1366
16. Cui X, Li CM, Bao H, Zheng X, Lu Z (2008) In situ fabrication of silver nanoarrays in hyaluronan/PDDA layer-by-layer assembled structure. J Colloid Interface Sci 327(2):459–465
17. Yu C, Zhou X, Gu H (2010) Immobilization, direct electrochemistry and electrocatalysis of hemoglobin on colloidal silver nanoparticles-chitosan film. Electrochim Acta 55(28):8738–8743
18. Zhao S, Zhang K, Sun Y, Sun C (2006) Hemoglobin/colloidal silver nanoparticles immobilized in titania sol-gel film on glassy carbon electrode: direct electrochemistry and electrocatalysis. Bioelectrochemistry 69(1):10–15
19. Lapčík L, De Smedt S, Demeester J, Chabreček P (1998) Hyaluronan: preparation, structure, properties, and applications. Chem Rev 98(8):2663–2684
20. Day AJ, Sheehan JK (2001) Hyaluronan: polysaccharide chaos to protein organisation. Curr Opin Struct Biol 11(5):617–622
21. Cowman MK, Matsuoka S (2005) Experimental approaches to hyaluronan structure. Carbohydr Res 340(5):791–809
22. Burke SE, Barrett CJ (2005) Swelling behavior of hyaluronic acid/polyallylamine hydrochloride multilayer films. Biomacromolecules 6(3):1419–1428
23. Picart C, Lavalle P, Hubert P, Cuisinier FJG, Decher G, Schaaf P, Voegel JC (2001) Buildup mechanism for poly(l-lysine)/hyaluronic acid films onto a solid surface. Langmuir 17(23):7414–7424
24. Liu H, Hu N (2006) Interaction between myoglobin and hyaluronic acid in their layer-by-layer assembly: quartz crystal microbalance and cyclic voltammetry studies. J Phys Chem B 110 (29):14494–14502
25. Barsan MM, Pinto EM, Brett CMA (2010) Interaction between myoglobin and hyaluronic acid in layer-by-layer structures—an electrochemical study. Electrochim Acta 55(22):6358–6366
26. Turner RFB, Harrison DJ, Rojotte RV (1991) Preliminary in vivo biocompatibility studies on perfluorosulphonic acid polymer membranes for biosensor applications. Biomaterials 12(4):361–368
27. Shi G, Liu M, Zhu M, Zhou T, Chen J, Jin L, Jin J-Y (2002) The study of Nafion/xanthine oxidase/Au colloid chemically modified biosensor and its application in the determination of hypoxanthine in myocardial cells in vivo. Analyst 127(3):396–400
28. Trewyn BG, Giri S, Slowing S, Lin SY (2007) Mesoporous silica nanoparticle based controlled release, drug delivery, and biosensor systems. Chem Commun 31:3236–3245
29. Cui X, Li CM, Bao H, Zheng X, Zang J, Ooi CP, Guo J (2008) Hyaluronan-assisted photoreduction synthesis of silver nanostructures: from nanoparticle to nanoplate. J Phys Chem C 112 (29):10730–10734
30. Matthew JB, Hanania GIH, Gurd FRN (1979) Coordination complexes and catalytic properties of proteins and related substances. 104. Electrostatic effects in hemoglobin: hydrogen ion equilibriums in human deoxy- and oxyhemoglobin A. Biochemistry 18(10):1919–1928
31. Yang L, Lee CS, Hofstadler SA, Pasa-Tolic L, Smith RD (1998) Capillary isoelectric focusing–electrospray ionization Fourier transform ion cyclotron resonance mass spectrometry for protein characterization. Anal Chem 70(15):3235–3241
32. He P, Hu N (2004) Interactions between heme proteins and dextran sulfate in layer-by-layer assembly films. J Phys Chem B 108(35):13144–13152
33. Liu H-H, Zou G-L (2006) Electrochemical investigation of immobilized hemoglobin: redox chemistry and enzymatic catalysis. J Biochem Bioph Methods 68(2):87–99
34. Miao X, Liu Y, Gao W, Hu N (2010) Layer-by-layer assembly of collagen and electroactive myoglobin. Bioelectrochemistry 79 (2):187–192
35. Wang Y-H, Gu H-Y (2009) Hemoglobin co-immobilized with silver–silver oxide nanoparticles on a bare silver electrode for hydrogen peroxide electroanalysis. Microchimica Acta 164(1):41–47
36. Xu Y, Hu C, Hu S (2008) A hydrogen peroxide biosensor based on direct electrochemistry of hemoglobin in Hb–Ag sol films. Sens Actuators, B 130(2):816–822
37. Murray RW (1986) Chemically modified electrodes. In: Bard AJ (ed) Electroanalytical chemistry, vol 13. Marcel Dekker, New York, pp 89–421
38. Wang S-F, Chen T, Zhang Z-L, Pang D-W, Wong K-Y (2007) Effects of hydrophilic room-temperature ionic liquid 1-butyl-3-

methylimidazolium tetrafluoroborate on direct electrochemistry and bioelectrocatalysis of heme proteins entrapped in agarose hydrogel films. Electrochem Commun 9(7):1709–1714
39. Zhao G, Xu J-J, Chen H-Y (2006) Fabrication, characterization of Fe_3O_4 multilayer film and its application in promoting direct electron transfer of hemoglobin. Electrochem Commun 8(1):148–154
40. Wang S-F, Chen T, Zhang Z-L, Shen X-C, Lu Z-X, Pang D-W, Wong K-Y (2005) Direct electrochemistry and electrocatalysis of heme proteins entrapped in agarose hydrogel films in room-temperature ionic liquids. Langmuir 21(20):9260–9266
41. Wen Y, Yang X, Hu G, Chen S, Jia N (2008) Direct electrochemistry and biocatalytic activity of hemoglobin entrapped into gellan gum and room temperature ionic liquid composite system. Electrochim Acta 54(2):744–748
42. Laviron E (1979) The use of linear potential sweep voltammetry and of a.c. voltammetry for the study of the surface electrochemical reaction of strongly adsorbed systems and of redox modified electrodes. J Electroanal Chem Interfacial 100(1–2):263–270
43. Laviron E (1979) General expression of the linear potential sweep voltammogram in the case of diffusionless electrochemical systems. J Electroanal Chem Interfacial Electrochem 101(1):19–28
44. Chen L, Lu G (2007) Novel amperometric biosensor based on composite film assembled by polyelectrolyte-surfactant polymer, carbon nanotubes and hemoglobin. Sens Actuators, B 121(2):423–429
45. Wyman J (1968) Regulation in macromolecules as illustrated by haemoglobin. Q Rev Biophys 1(01):35–80
46. Bond AM (1980) Modern polarographic methods in analytical chemistry. Marcel Dekker, New York
47. Yamazaki I, Araiso T, Hayashi Y, Yamada H, Makino R (1978) Analysis of acid-base properties of peroxidase and myoglobin. Adv Biophys 11:249–281
48. Yin Y, Zhang H, Nishinari K (2007) Voltammetric characterization on the hydrophobic interaction in polysaccharide hydrogels. J Phys Chem B 111(7):1590–1596
49. Jiang H, Du C, Zou Z, Li X, Akins D, Yang H (2009) A biosensing platform based on horseradish peroxidase immobilized onto chitosan-wrapped single-walled carbon nanotubes. J Solid State Electrochem 13(5):791–798
50. Xu J, Liu C, Wu Z (2011) Acerate ZnO whiskers and sodium alginate films: preparation and application in bioelectrochemistry of hemoglobin. J Solid State Electrochem 1–6
51. Zeng X, Wei W, Li X, Zeng J, Wu L (2007) Direct electrochemistry and electrocatalysis of hemoglobin entrapped in semi-interpenetrating polymer network hydrogel based on polyacrylamide and chitosan. Bioelectrochemistry 71(2):135–141
52. Xu J, Shang F, Luong JHT, Razeeb KM, Glennon JD (2010) Direct electrochemistry of horseradish peroxidase immobilized on a monolayer modified nanowire array electrode. Biosens Bioelectron 25(6):1313–1318
53. Jamal M, Xu J, Razeeb KM (2010) Disposable biosensor based on immobilisation of glutamate oxidase on Pt nanoparticles modified Au nanowire array electrode. Biosens Bioelectron 26(4):1420–1424
54. Lu Q, Hu S (2006) Studies on direct electron transfer and biocatalytic properties of hemoglobin in polytetrafluoroethylene film. Chem Phys Lett 424(1–3):167–171
55. Xu H, Dai H, Chen G (2010) Direct electrochemistry and electrocatalysis of hemoglobin protein entrapped in graphene and chitosan composite film. Talanta 81(1–2):334–338
56. Zheng W, Li J, Zheng YF (2008) An amperometric biosensor based on hemoglobin immobilized in poly(ε-caprolactone) film and its application. Biosens Bioelectron 23(10):1562–1566
57. Yu J, Ju H (2003) Amperometric biosensor for hydrogen peroxide based on hemoglobin entrapped in titania sol–gel film. Anal Chim Acta 486(2):209–216
58. Yabuki S, Mizutani F, Hirata Y (2000) Hydrogen peroxide determination based on a glassy carbon electrode covered with polyion complex membrane containing peroxidase and mediator. Sens Actuators, B 65(1–3):49–51